Exact Solutions in Attitude Dynamics of a Magnetic Dual-Spin Spacecraft and a Generalization of the Lagrange Top

ANTON V. DOROSHIN
Space Engineering Department (Division of Flight Dynamics and Control Systems)
Samara State Aerospace University (National Research University)
SSAU, Moscowskoe shosse 34, Samara, Russia 443086
RUSSIAN FEDERATION
doran@inbox.ru

Abstract: - The present paper contains an investigation results for the attitude motion of a magnetic dual-spin spacecraft (DSSC) in the geomagnetic field at the realization of the orbital motion of its mass center along an equatorial circular orbit. Exact analytical solutions for the attitude motion parameters are obtained in the elliptic Jacobi functions including the angular momentum components, the directional cosines and the Euler angles. These analytical exact solutions correspond to generating dependences which make possible the advanced research of the DSSC perturbed motion cases. The considering task of the DSSC angular motion can be characterized as the Lagrange top generalization for the coaxial bodies system – the corresponding case of the magnetic DSSC motion occurs under the influence of external restoring/overturning torques (like in the Lagrange heavy top motion). This paper's results also can be directly reduced to the Euler coaxial top's (Euler's case of the rigid body and coaxial bodies motion) general exact explicit solutions; this circumstance can be consider as a generalization of the Euler coaxial top's problem. An important "dynamical equivalence" between the magnetic and gyroscopic DSSC attitude stabilization factors is illustrated.

Key-Words: - Magnetic Dual-Spin Spacecraft; Explicit Solutions; Jacobi Functions; Lagrange top; Euler top

1 Introduction

The study of various aspects of the attitude/angular motion of a dual-spin spacecraft (DSSC) and gyrostat-satellites still remains one of the important parts of modern orbital dynamics and spacecraft attitude dynamics. This research area is closely connected with classical tasks of the rigid bodies' angular motion [1-6]. Regular and irregular (chaotic) motion modes, the attitude control of gyrostats and a coaxial spacecraft are being examined by many scientists [7-40]. Important research results corresponding to the rigid body and gyrostats motion are presented in many papers, for example, in [1-7]. In [8, 9] the torque-free motion dynamics of the gyrostats is studied.

An analysis of the angular motion of coaxial bodies and the dual-spin spacecraft in different problem formulations was conducted, for example, in [10-20] including perturbed motion regimes. In [16-19] investigation results for the DSSC attitude motion at the rotor-body spinup maneuver realization were collected. In [20-33] the gyrostats/DSSC compound motion modes were considered at the absence/presence of perturbations and control torques.

The attitude dynamics/control of the magnetic spacecraft was considered, for example, in [26-33]. New aspects of the angular motion of a satellite equipped with the active magnetic attitude control system were examined in [27].

In [34, 35] the angular motion of the variable mass dual-spin spacecraft was investigated. The mass changing in [34, 35], first of all, is connected with the solid propellant engine operating of the DSSC which implements an interorbital transfer maneuver [e.g. 40]. The attitude motion of the DSSC with the operating engine at nonzero values of angles of the nutation and the precession can increase a final error of the transfer impulse (due to sputtering of the engine thrust) – it leads to an error in the final orbit.

In the paper [36] the gyrostats' chaotic motion in resistant environments was considered based on the well-known dynamical systems with strange attractors (e.g. Lorenz, Rössler, Newton–Leipnik and Sprott attractors). In [37, 38] the local heteroclinic chaotization of the torque-free dual-spin spacecraft was examined with the help of the Melnikov and Wiggins methods.

In [39] the coaxial Lagrange top was fully considered in the case of the dynamical symmetry of both coaxial bodies.

In other words, the problem of the DSSC attitude dynamics is the wide independent area of the spaceflight and classical mechanics, which includes many important aspects of the unperturbed/perturbed motion under influence of different external/internal disturbances. But especially we should emphasize the analytical study problem.

Analytical exact solutions play the particular role in the motion analysis (and also in the synthesis). The analytical exact solutions make possible the advanced investigation of the motion features – we can use these solution as the generating solutions for the perturbed modes study, including the irregular/chaotic behavior of systems [41-45]. The important analytical investigations of the rigid body/DSSC/gyrostat motion are presented in [1-12].

In this paper the analytical exploration of the attitude dynamics problems with the focus on the magnetic DSSC motion investigation under influence of the constant magnetic field is continued – this case describes the attitude motion of the magnetic DSSC in the geomagnetic field at the realization of the orbital motion of its mass center along an equatorial circular orbit. This regime of the magnetic DSSC angular motion is quite important for the practice because it corresponds (in ideal conditions) to one of the preferred regimes of the stationary attitude motions with the conservation of the spatial orientation of the longitudinal axes of the satellite (and especially the communication satellite) – these regimes represent so-called "cylindrical precessions" of the spin-stabilized satellites. As a part of the article research results we can indicate the consideration of the "dynamical symmetry/equivalence" between the magnetic and gyroscopic DSSC attitude stabilization factors.

Also it is very important to underline that the task of the magnetic DSSC attitude motion is connected with such classical problems of the rigid body mechanics like the integrable cases of rigid body angular motion (the Euler, the Lagrange and the Kovalevskaya tops).

2 The angular motion equations of the magnetic DSSC and the coaxial Lagrange top

Let us consider the attitude dynamics of the DSSC (coaxial bodies) which include the internal permanent magnet or the current-carrying inductive coil (with the magnetic dipole moment **m**) under the influence of the external restoring/overturning torque $\mathbf{M}_\theta$ from the magnetic field. Assume that the DSSC's mass center is moved on the circular equatorial orbit of the Earth which has the ideal single dipole magnetic field; the corresponding to this equatorial orbit magnetic field vector we denote as $\mathbf{B}_{\mathbf{orb}}$ (Fig.1-a). It is needed to underline that in this case along the whole circle equatorial orbit magnetic vector $\mathbf{B}_{\mathbf{orb}}$ is constant and orthogonal to the orbit plane (Fig.1) ($\mathbf{B}_{\mathbf{orb}}$ is the tangent vector to the surface of the magnetic field (Fig.1-b); the magnitude of this vector corresponds to the altitude of the circle orbit).

The DSSC consist from two coaxial bodies (body #1 is a rotor; body #2 is a main/core/carrier body). The rotor-body rotates in the inertial space with an angular velocity $\boldsymbol{\omega}_1$, and the main carrier body rotates with an angular velocity $\boldsymbol{\omega}_2$. The angular velocity of the rotor-body differs from the angular velocity of the main carrier body on a vector of a relative rotation angular velocity $\boldsymbol{\sigma}$ about a common longitudinal DSSC axes ($\boldsymbol{\omega}_1 = \boldsymbol{\omega}_2 + \boldsymbol{\sigma}$).

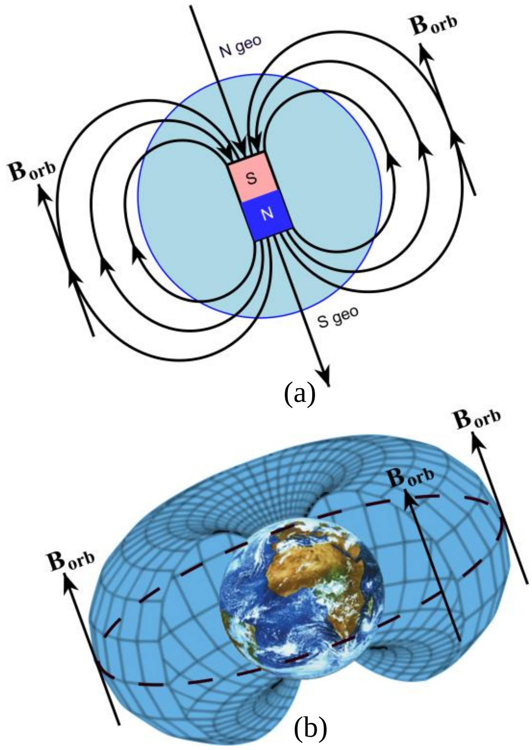

Fig.1 *Single dipole model of the Earth's magnetic field (a) and the constant magnetic field vector corresponding to the circle equatorial orbit (b)*

Let us introduce the following coordinate frames (Fig.2-a): *OXYZ* is the inertial system of coordinates, where the axis *OZ* is collinear with the constant magnetic vector (**k'** is the unit vector of the *OZ* axis) and then $\mathbf{B}_{\mathbf{orb}} = B_{orb}\mathbf{k}'$; $Ox_2y_2z_2$ is the connected principal system of coordinates of the carrier body (**i**, **j**, **k** are the corresponding unit vectors); and $Ox_1y_1z_1$ – the connected principal system of coordinates of the rotor body. The vectors $\mathbf{k}$, $\mathbf{k'}$ are the unit vectors of the axes *OZ* and Oz_2 respectively.

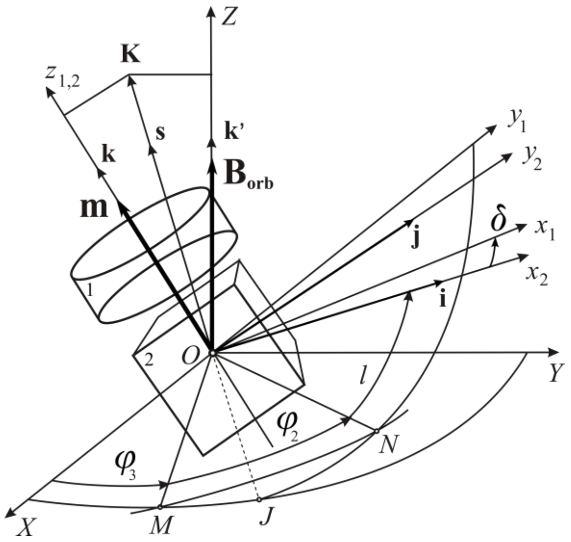

(a)

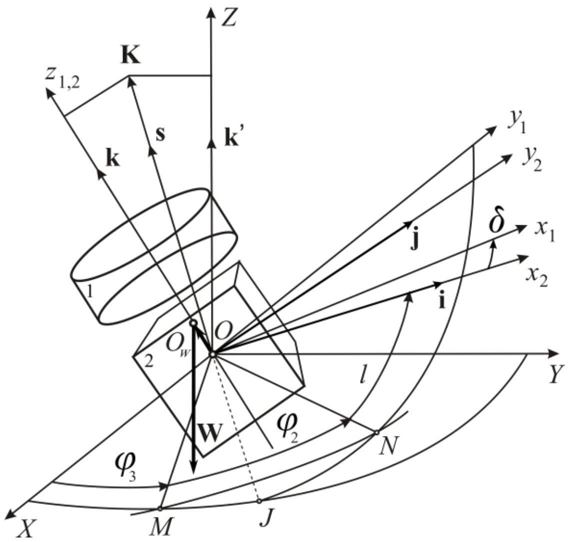

(b)

Fig.2 *The magnetic DSSC coordinate frames (a) and the "heavy coaxial top" (b) with the Andoyer–Deprit coordinates*

The axes Oz_1 and Oz_2 of the connected systems are identical to the common longitudinal rotation axis of the DSSC coaxial bodies. We assume that the main body has a triaxial inertia tensor and the rotor is a dynamically symmetrical body, and that the DSSC intrinsic permanent magnet is aligned with the DSSC's longitudinal axis $(\mathbf{m} = m\mathbf{k})$.

The system motion can be described on the base of the Euler dynamical equations [3-5], which correspond to the angular momentum changing low/theorem writing in an arbitrary rotating coordinate fame

$$\dot{\mathbf{K}} + \boldsymbol{\Omega} \times \mathbf{K} = \mathbf{M}^{\mathbf{e}} \tag{1}$$

where $\mathbf{K}$ is the system angular momentum, $\boldsymbol{\Omega}$ is the angular velocity of the "selected rotating coordinate frame" (it can be differ from the bodies coordinate frames), $\mathbf{M}^{\mathbf{e}}$ – is the vector of external torques.

Usually the bodies' connected coordinate frames are used for the dynamical equations construction as the "selected rotating coordinate frames" (and, consequently, we will use the carrier body's frame, then $\boldsymbol{\Omega} = \boldsymbol{\omega}_2$). Therefore, we obtain the dynamical Euler equations of the motion in projections on the axes of the DSSC main carrier body frame $Ox_2y_2z_2$:

$$\begin{cases} A\dot{p} + (C - B)qr + qC_1\sigma = M_{\theta x} \\ B\dot{q} + (A - C)pr - pC_1\sigma = M_{\theta y} \\ C\dot{r} + C_1\dot{\sigma} + (B - A)pq = M_{\theta z} \\ C_1(\dot{r} + \dot{\sigma}) = M_\Delta \end{cases} \tag{2}$$

where $\{p, q, r\}$ are the components of the carrier body's angular velocity $\boldsymbol{\omega}_2$ in projections onto the axes of the $Ox_2y_2z_2$ frame; σ is the rotor angular velocity relatively the carrier body $(\sigma = \dot{\delta})$; $\mathbf{I}_2 = diag[A_2, B_2, C_2]$ is the triaxial inertia tensor of the carrier body in the connected frame $Ox_2y_2z_2$; $\mathbf{I}_1 = diag[A_1, A_1, C_1]$ is the inertia tensor of the dynamically symmetrical rotor in the connected frame $Ox_1y_1z_1$; $A = A_1 + A_2$, $B = A_1 + B_2$, $C = C_1 + C_2$ are the main inertia moments of the coaxial bodies system in the frame $Ox_2y_2z_2$ (including rotor); $\Delta = C_1(r + \sigma) -$ the longitudinal angular moment of the rotor along Oz_1; $C_1\sigma = h_{z_1} -$ the rotor relative angular moment in the carrier body frame $Ox_2y_2z_2$. $M_\Delta -$ is the internal torque of the coaxial bodies interaction (we assume $M_\Delta = 0$).

The torque from the magnetic field influence is

$$\mathbf{M}_\theta = \mathbf{m} \times \mathbf{B}_{\mathbf{orb}};$$

$$\mathbf{M}_\theta\big|_{Ox_2y_2z_2} = \left[M_{\theta x}, M_{\theta y}, M_{\theta z}\right]^T = \tag{3}$$

$$= \left[-B_{orb}m\gamma_2, B_{orb}m\gamma_1, 0\right]^T$$

The parameters γ_i in the vector expression (3) are the direction cosines of the inertial axis *OZ* in the main body frame $Ox_2y_2z_2$:

$$\begin{aligned}\gamma_1 &= \mathbf{i}\cdot\mathbf{k'} = \cos\left(OZ, Ox_2\right),\\ \gamma_2 &= \mathbf{j}\cdot\mathbf{k'} = \cos\left(OZ, Oy_2\right),\\ \gamma_3 &= \mathbf{k}\cdot\mathbf{k'} = \cos\left(OZ, Oz_2\right)\end{aligned} \tag{4}$$

Also equations (1) can be presented in the following form:

$$\begin{aligned}&A\dot{p} + \left(C_2 - B\right)qr + q\Delta = -Q\gamma_2;\\ &B\dot{q} + \left(A - C_2\right)pr - p\Delta = Q\gamma_1;\\ &C_2\dot{r} + \dot{\Delta} + \left(B - A\right)pq = 0;\quad \dot{\Delta} = M_\Delta\end{aligned} \tag{5}$$

where $Q = B_{orb}m$.

We assume the following conditions:

$$A_2 > B_2 > C_2 > A_1 > C_1,\quad \Delta = \text{const} > 0.$$

Also it is needed to note that kinematical equations should be added to description of the angular motion – we can use as these equations the well-known Poisson equations for directional cosines of the inertial axes in the body frame.

Here we note that the equation system (1) corresponds to the motion of the coaxial bodies and the unbalanced gyrostat with non-constant relative angular moment of rotor ($h_{z_1} = C_1\sigma \neq \text{const}$, even if $M_\Delta = 0$). In this case results of the analysis for the Kelvin-type gyrostats [1-4, 7-8] are not applicable.

Also we can use the Hamiltonian form of equations in the Andoyer–Deprit canonical variables. The Andoyer–Deprit variables [6, 9, 10, 13, 14, 37, 38] (l, L, I_2, I_3) can be expressed with the help of the coaxial system's angular momentum $\mathbf{K} = \mathbf{K}\big|_{Ox_2y_2z_2} = \left[K_{x_2}, K_{y_2}, K_{z_2}\right]^T$ (Fig.2):

$$\begin{aligned}&L = \frac{\partial T}{\partial \dot{l}} = \mathbf{K}\cdot\mathbf{k};\\ &I_2 = \frac{\partial T}{\partial \dot{\varphi}_2} = \mathbf{K}\cdot\mathbf{s} = \left|\mathbf{K}\right| = K;\\ &I_3 = \frac{\partial T}{\partial \dot{\varphi}_3} = \mathbf{K}\cdot\mathbf{k}';\quad L \le I_2\end{aligned} \tag{6}$$

$$\begin{aligned}&K_{x_2} = Ap = \sqrt{I_2^2 - L^2}\sin l;\\ &K_{y_2} = Bq = \sqrt{I_2^2 - L^2}\cos l;\\ &K_{z_2} = C_2 r + \Delta = L\end{aligned} \tag{7}$$

The system Hamiltonian [9, 37, 38] in the Andoyer–Deprit phase space takes the form:

$$\mathcal{H} = T + P + \varepsilon\mathcal{H}_1$$

$$T = \frac{I_2^2 - L^2}{2}\left[\frac{\sin^2 l}{A_1 + A_2} + \frac{\cos^2 l}{A_1 + B_2}\right] + \frac{1}{2}\left[\frac{\Delta^2}{C_1} + \frac{\left(L - \Delta\right)^2}{C_2}\right], \tag{8}$$

where T – is the system kinetic energy; P – is the potential energy depending on the type of the external/internal influence; $\varepsilon\mathcal{H}_1$ – is the small perturbed part of the Hamiltonian, connected with small disturbances. In our case the potential energy corresponds to the restoring/overturning torque (from the magnetic field or from the system's weight) and takes the form depending only on the nutation angle [3, 5]:

$$P = Q\cos\theta;\quad M_\theta = -\frac{\partial P}{\partial \theta} = Q\sin\theta \tag{9}$$

At the end of this section we also underscore the full compliance of the mechanical models (Fig.2) of the considering magnetic DSSC motion and the coaxial Lagrange top (the heavy coaxial top) motion (Fig.2-b). The Lagrange top in the classical description [5, 6] characterizes the angular motion of the heavy body about fixed point O when the gravity force $\mathbf{W}$ (the system weight) is applied in the point O_W on the general longitudinal axis Oz_2. Our models (the magnetic DSSC and the heavy coaxial top) can be reduced to the interconnected case at performing of the following notations:

$$Q = B_{orb}m;\qquad Q = -W\left|OO_W\right|; \tag{10}$$

The notations (10) also underline the common type of the external influence in the considering cases; but in the case of the magnetic DSSC the corresponding magnetic torque is restoring and in the case of the heavy coaxial top the gravity torque is overturning.

Here it is worth to note that in [39] the coaxial Lagrange top (CLT) was fully considered in the case of the dynamical symmetry of both bodies (the carrier and the rotor): the fourth integral of the motion (which is necessary for the problem solving) were written [39] for the CLT at the presence of the arbitrary internal torque M_Δ – it allowed to obtain the exact explicit solutions for all of the Euler angles (it is needed to underline that the exact explicit solutions in the form of elliptic integrals of the third kind [39] were obtained by V.S. Aslanov using approaches [10]); also Larmor's precession was indicated as the possible motion regime of the CLT, and the "lunar motion" case was investigated. In the continuation of the Lagrange top generalization we consider in this paper the motion of the CLT with the general triaxial inertia tensor of the main body in the important case when the system angular momentum $\mathbf{K}$ is directed precisely along the inertial axis OZ coinciding with the vector of the external force field $\left(\mathbf{B_{orb}} \text{ or } \mathbf{W}\right)$.

3 Explicit analytical solutions for angular momentum components

Let us consider the angular motion of the magnetic DSSC (and the coaxial Lagrange top) with the respect to the initial frame *OXYZ* (Fig.2) in the case when the vector of the angular momentum **K** is directed along the inertial axis *OZ* $(\mathbf{K}=K\,\mathbf{k'})$ coinciding with the vector of the external force field $(\mathbf{B_{orb}};\ \mathbf{W})$. Also we assume the absence of the internal coaxial bodies interaction $(M_\Delta=0)$ and, consequently, the constancy of the rotor angular momentum Δ. This case of the motion of the magnetic DSSC is quite important because it corresponds (in ideal conditions) to one of the preferred regimes of the stationary motions of spin-stabilized satellites in the orbit – these regimes represent so-called "cylindrical precessions" of the spin-stabilized satellites.

In this case the system angular momentum K is constant, and we have the following expressions (4) for the directional cosines of the *OZ* axis, for Andoyer–Deprit momentums (6) and for the nutation angle:

$$\gamma_1=\frac{K_{x_2}}{K}=\frac{Ap}{K},\quad \gamma_2=\frac{K_{y_2}}{K}=\frac{Bq}{K},\quad \gamma_3=\frac{K_{z_2}}{K}=\frac{C_2r+\Delta}{K} \tag{11}$$

$$L=K_{z_2}=C_2r+\Delta;\quad I_2=I_3=K=\text{const};\quad \cos\theta=\frac{K_{z_2}}{K}=\frac{L}{K}=\frac{C_2r+\Delta}{K}, \tag{12}$$

The vector of the magnetic torque in considering case takes the form

$$\mathbf{M_0}\big|_{Ox_2y_2z_2}=\left[\frac{-QK_{x_2}}{K},\frac{QK_{y_2}}{K},0\right]^T=\left[\frac{-QAp}{K},\frac{QBq}{K},0\right]^T \tag{13}$$

Then the dynamical motion equation (5) can be rewritten in the form

$$\begin{aligned}&A\dot p+(C_2-B)qr+q\Delta=-QBq/K;\\ &B\dot q+(A-C_2)pr-p\Delta=QAp/K;\\ &C_2\dot r+\dot\Delta+(B-A)pq=0;\quad \dot\Delta=M_\Delta\end{aligned} \tag{14}$$

Let us obtain the analytical solutions for all of the angular velocity components {p, q, r, σ} by analogy with the previous results [12].

In the purpose of the exact solutions obtaining we will use the polhodes geometry [3, 12]. The polhode is the fourth-order curve in 3D-space (Fig.3) corresponding to the intersection of a kinetic energy ellipsoid and an angular momentum ellipsoid, which are defined with the help of the expressions for the dynamical theorems/laws of the changing of the kinetic energy and the angular momentum [3]:

$$Ap^2+Bq^2+C_2r^2+\frac{\Delta^2}{C_1}-2T_0==2P(\theta)-2P(\theta_0) \tag{15}$$

$$A^2p^2+B^2q^2+[C_2r+\Delta]^2=K^2 \tag{16}$$

The expressions (15) and (16) with the help of (9) and (12) can be rewritten

$$Ap^2+Bq^2+C_2r^2+\frac{\Delta^2}{C_1}+2E(C_2r+\Delta)=2\tilde T \tag{17}$$

$$A^2p^2+B^2q^2+[C_2r+\Delta]^2=K^2=2D\tilde T \tag{18}$$

where the following constants take place

$$2T_0=Ap_0^2+Bq_0^2+C_2r_0^2+\frac{\Delta^2}{C_1};\quad \tilde T=T_0-Q\frac{C_2r_0+\Delta}{K}=\text{const};\quad E=-\frac{Q}{K};\quad D=\frac{K^2}{2\tilde T} \tag{19}$$

Based on the expressions (17) and (18) combinations (the multiplication of (17) by A and the deduction of (18)) we can write the expression:

$$B(A-B)q^2+ +A\left(C_2r^2+\frac{\Delta^2}{C_1}+2E[C_2r+\Delta]\right)- -[C_2r+\Delta]^2=2\tilde T(A-D) \tag{20}$$

The multiplication of (17) by B with the deduction of (18) gives

$$A(B-A)p^2+ +B\left(C_2r^2+\frac{\Delta^2}{C_1}+2E[C_2r+\Delta]\right)- -[C_2r+\Delta]^2=2\tilde T(B-D) \tag{21}$$

The allocating of a perfect square in (21) gives us the equation for hyperbolae (on the coordinate plane *Opr* at the Fig.3)

$$-A(A-B)p^2+ +C_2(B-C_2)\left[r-\frac{\Delta-EB}{B-C_2}\right]^2=F \tag{22}$$

where

$$F = 2\tilde{T}(B-D) + \frac{C_2}{B-C_2}(\Delta - EB)^2 - \left[\left(\frac{B}{C_1}-1\right)\Delta^2 + 2EB\Delta\right] \quad (23)$$

The allocating of a perfect square in (20) gives us the equation for ellipses (on the coordinate plane *Oqr* at the Fig.3)

$$B(A-B)q^2 + C_2(A-C_2)\left[r - \frac{\Delta - EA}{A-C_2}\right]^2 = H \quad (24)$$

$$H = 2\tilde{T}(A-D) + \frac{C_2}{A-C_2}(\Delta - EA)^2 - \left[\left(\frac{A}{C_1}-1\right)\Delta^2 + 2EA\Delta\right] \quad (25)$$

From the equation (22) we can obtain

$$p = \pm\sqrt{\frac{C_2(B-C_2)\left[r - \frac{\Delta - EB}{B-C_2}\right]^2 - F}{A(A-B)}} \quad (26)$$

From (24) we can get

$$r - \frac{\Delta - EA}{A-C_2} = \pm\sqrt{\frac{H - B(A-B)q^2}{C_2(A-C_2)}} \quad (27)$$

With the help of (27) we can write the auxiliary expression

$$r - \frac{\Delta - EB}{B-C_2} = \pm\sqrt{\frac{H - B(A-B)q^2}{C_2(A-C_2)}} - \Delta\beta - E\alpha; \quad (28)$$

$$\alpha = \frac{A}{A-C_2} - \frac{B}{B-C_2};$$

$$\beta = \frac{1}{B-C_2} - \frac{1}{A-C_2}$$

Based on the expressions (11) we can rewrite the second equation (5)

$$B\dot{q} + (A-C_2)pr - p\Delta = -EAp$$

Taking into account (28), (26) the last equation can be written in the form

$$B\dot{q} = \mp(A-C_2) f_1(q) f_2(q);$$

$$f_1(q) = \sqrt{\frac{C_2(B-C_2)}{A(A-B)}\left[\pm V - \Delta\beta - E\alpha\right]^2 - \frac{F}{A(A-B)}};$$

$$f_2(q) = V; \qquad V = \sqrt{\frac{H - B(A-B)q^2}{C_2(A-C_2)}} \quad (29)$$

We can make the change of variables (case 1)

$$x = +\sqrt{\frac{H - B(A-B)q^2}{C_2(A-C_2)}} - \Delta\beta - E\alpha \quad (30)$$

Then from (30) we obtain

$$(x + \Delta\beta + E\alpha)^2 = \frac{H - B(A-B)q^2}{C_2(A-C_2)} \quad (31)$$

$$\begin{cases} q = \pm\sqrt{\dfrac{H - C_2(A-C_2)(x+\Delta\beta+E\alpha)^2}{B(A-B)}}; \\ dq = \mp\dfrac{C_2(A-C_2)}{B(A-B)}\dfrac{(x+\Delta\beta+E\alpha)dx}{\sqrt{\dfrac{H - C_2(A-C_2)(x+\Delta\beta+E\alpha)^2}{B(A-B)}}} \end{cases} \quad (32)$$

Also we can make the following change of variables (case 2)

$$x = -\sqrt{\frac{H - B(A-B)q^2}{C_2(A-C_2)}} - \Delta\beta - E\alpha \quad (33)$$

As in the previous case (30), from (33) expressions (31) and (32) follow again. So, for both changes we have the interconnected equation

$$dt = \pm\frac{M\,dx}{\sqrt{H - a(x+b)^2}\sqrt{cx^2 - G}} \quad (34)$$

where

$$M = C_2\sqrt{\frac{B}{A-B}}; \quad G = \frac{F}{A(A-B)};$$

$$a = C_2(A-C_2); \; b = \Delta\beta + E\alpha; \quad (35)$$

$$c = \frac{C_2(B-C_2)}{A(A-B)}$$

We should note differences between the initial values corresponding to the cases (i=1, 2):

$$x(t_0) = x_i^{ini} = (-1)^{i+1}\sqrt{\frac{H - B(A-B)q_0^2}{C_2(A-C_2)}} - \Delta\beta - E\alpha; \quad i = 1, 2$$

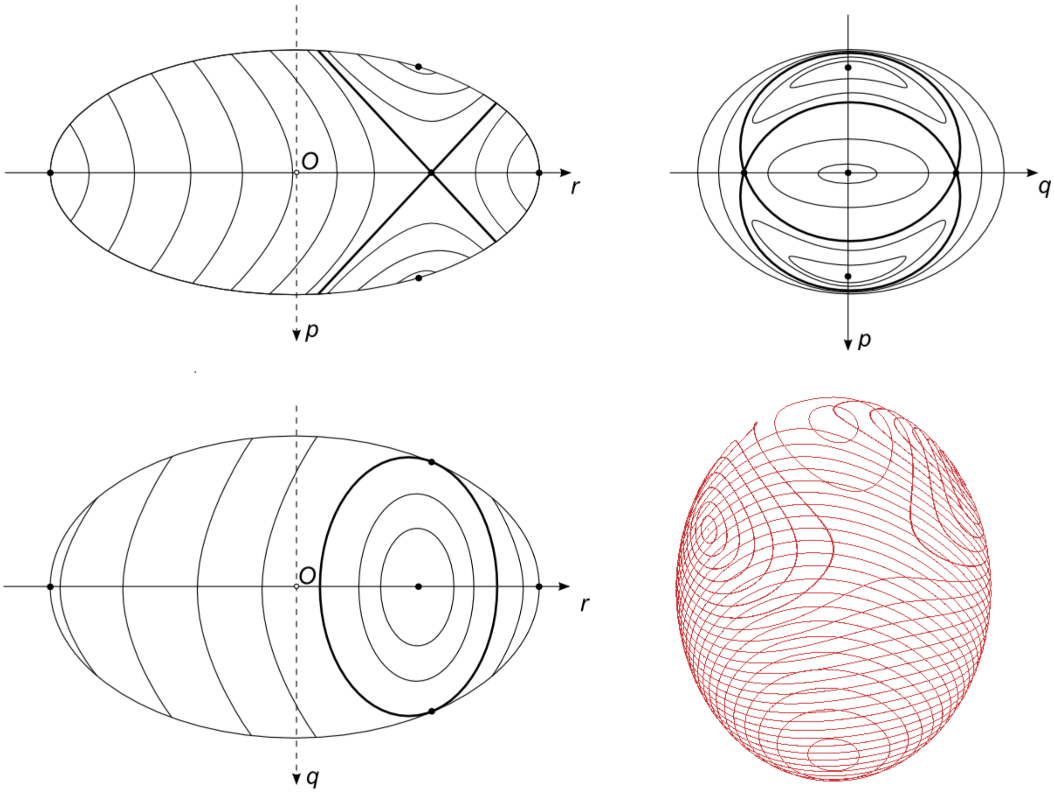

Fig.3 *The polhodes ellipsoid*

By full analogy with [12] we rewrite the equation (34) in the form with differences of squares

$$dt = \pm \frac{M}{\sqrt{ac}} \frac{dx}{\sqrt{\left(\sqrt{\frac{H}{a}}\right)^2 - (x+b)^2} \sqrt{x^2 - \left(\sqrt{\frac{G}{c}}\right)^2}} \tag{36}$$

The next change of the variables can be used

$$z = \sqrt{\frac{R(x-e)}{P(x+e)}}$$

$$R = -b - d + e; \quad P = -b - d - e \tag{37}$$

$$d = \sqrt{H/a}; \quad e = \sqrt{G/c}$$

Then based on (37) we express relations

$$x = \frac{-R/P - z^2}{-R/P + z^2} e; \qquad dx = \frac{R}{P} \frac{4ez\,dz}{\left(-R/P + z^2\right)^2} \tag{38}$$

The substitution of (38) into the equation (36) gives us

$$dt = \pm \frac{4eMR}{P\sqrt{ac}\sqrt{\frac{H}{a}\left(z^2 - \frac{R}{P}\right)^2 - \left(e\left[\frac{-R}{P} - z^2\right] + b\left[z^2 - \frac{R}{P}\right]\right)^2}} \cdot$$

$$\cdot \frac{zdz}{\sqrt{e^2\left(\frac{-R}{P} - z^2\right)^2 - \frac{G}{c}\left(z^2 - \frac{R}{P}\right)^2}}$$

The last equation also can be written in the form

$$dt = \pm 2eM \frac{\sqrt{R/P}}{\sqrt{aG}} \left[\sqrt{s_2 s_4}\sqrt{\left(1 - \frac{z^2}{c_1^2}\right)\left(1 - \frac{z^2}{c_2^2}\right)}\right]^{-1} dz$$

$$s_1 = \sqrt{\frac{H}{a}} + e - b; \quad s_2 = \frac{R}{P}\left[\sqrt{\frac{H}{a}} - e - b\right]$$

$$s_3 = \sqrt{\frac{H}{a}} - e + b; \quad s_4 = \frac{R}{P}\left[\sqrt{\frac{H}{a}} + e + b\right]$$

$$c_1^2 = s_2/s_1; \qquad c_2^2 = s_4/s_3 \tag{39}$$

We should consider two cases of the reduction of (39) to the elliptic integral of the first kind:

1). If $c_1 < c_2$ then the following substitution is efficient: $z = c_1 y$ and, moreover, $k = c_1/c_2 < 1$.

2). If $c_1 > c_2$ then: $z = c_2 y$ and $k = c_2/c_1 < 1$.

The equation (39) is rewritten

$$dt = \pm 2eM \frac{\sqrt{R/P}}{\sqrt{aG}} \frac{c_j dy}{\sqrt{s_2 s_4}\sqrt{(1-y^2)(1-k^2y^2)}}; \quad (40)$$

$j = 1,2$

where the index j corresponds to the number of the reduction case.

After the integration we obtain

$$\pm\left[N(t-t_0)+I_0\right] = \int_0^y \frac{dy}{\sqrt{(1-y^2)(1-k^2y^2)}};$$

$$N = \left[2eM \frac{c_j\sqrt{R/P}}{\sqrt{aG}\sqrt{s_2 s_4}}\right]^{-1}; \quad (41)$$

$$I_0 = \int_0^{y_0} \frac{dy}{\sqrt{(1-y^2)(1-k^2y^2)}} = \mathrm{const}$$

The inversion of the elliptic integral gives the explicit solution

$$y(t) = \mathrm{sn}\left[\pm\left(N(t-t_0)+I_0\right),k\right] \quad (42)$$

where sn(u,k) is the Jacobi elliptic sine function with the classical definition:

$$u = \Phi(\varphi) = \int_0^{\varphi} \frac{d\vartheta}{\sqrt{1-k^2\sin^2(\vartheta)}};$$

$$\varphi = \varphi(u) = \Phi^{-1}(u);$$

$$\mathrm{sn}(u,k) = \sin(\varphi(u));$$

Inverse transformations allow to obtain the exact explicit solutions for all angular velocity components

$$\begin{cases} q(t) = \pm\sqrt{\dfrac{1}{B(A-B)}\left[H - C_2(A-C_2)\left(x(t)+S\right)^2\right]} \\ p(t) = \pm\sqrt{\dfrac{1}{A(A-B)}\left[C_2(B-C_2)x^2(t) - F\right]} \\ r(t) = \dfrac{\Delta - EA}{A-C_2} \pm \left(x(t)+S\right); \qquad \sigma(t) = \dfrac{\Delta}{C_1} - r(t) \end{cases} \quad (43)$$

where

$$x(t) = e\frac{R/P + c_i^2\,\mathrm{sn}^2\left[\pm\left(N(t-t_0)+I_0\right),k\right]}{R/P - c_i^2\,\mathrm{sn}^2\left[\pm\left(N(t-t_0)+I_0\right),k\right]}; \quad (44)$$

$$S = \Delta\beta + E\alpha$$

Fig. 4 demonstrates the validity of solutions (43) - we see the comprehensive coincidence of the analytical (points) and the numerical integration[1] results (lines).

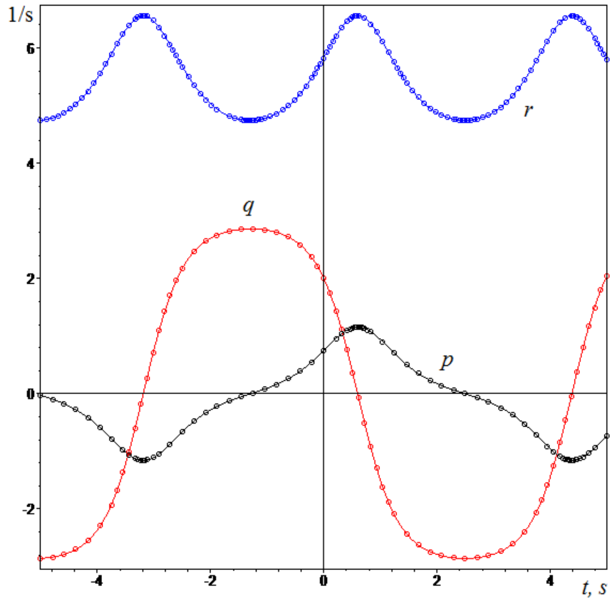

Fig.4 *The numerical integration (lines) and analytical (points) results*

A_2=15, B_2=8, C_2=6, A_1=5, C_1=4 [kg·m^2];

p_0=0.75, q_0=2, r_0=5.83 [1/s];

$\Delta = 5$, K=50 [kg·m^2/s]; Q=100 [kg·m^2/s^2]

Here we should note the analogy between the new results (43) and the torque-free DSSC motion solutions [12][2]. The difference of the results is defined by the presence of the additional rotational effect (it is described by the corresponding term $E\alpha$). This effect is connected with the magnetic field influence on the magnetic DSSC. Moreover, in the investigated case of the magnetic DSSC attitude motion this effect can be considered as the tantamount stabilizing factor (S) in comparison with the gyroscopic stabilization by the partial twist of the DSSC's rotors (with the relative angular velocity σ): we can simulate the gyroscopic stabilization as the magnetic stabilization (and vice versa) with the help of parameters Δ and E variation; also we can fully compensate the mutual actions of the magnetic and gyroscopic torques at $E\alpha = -\Delta\beta$.

So, based on the indicated equality of the magnetic and gyroscopic parts in the cumulative

[1] The numerical integration was fulfilled in the well known mathematical software MAPLE 11 using an *Implicit Rosenbrock third-fourth order Runge-Kutta* method with degree three interpolant.

[2] The article [12] contains the misprint in the expression (2.27): the multiplier c_i^2 before elliptic function sn^2(·) was missed in the numerator and in the denominator of the expression (2.27).

stabilizing factor S we can consider the torque-free attitude DSSC motion as the attitude motion of the magnetic spacecraft on the equatorial circular orbit at the coincidence of the angular momentum vector with the vector of the magnetic field (the normal to the orbit plane). It defines the important "dynamical equivalence" between two cases of the DSSC attitude motion. Also we ought to underline that the solutions for the magnetic coaxial bodies (DSSC, gyrostats) attitude/angular motion (43) generalize the well-known results for the torque-free rigid bodies/gyrostats in the Euler case of motion [1-12].

4 Explicit analytical solutions for kinematical parameters

Let us consider the kinematical aspects of the angular motion of the magnetic coaxial system (DSSC) with the respect to the initial frame $OXYZ$ (Fig.2) in the case when the vector of the angular momentum $\mathbf{K}$ is directed along OZ which coincides with the vector of the magnetic field $\mathbf{B_{orb}}$.

As it was indicated in the section 2 we are able to use the expressions (11) for the directional cosines, which are the main parameters describing the attitude of the DSSC in the inertial space $OXYZ$. Therefore, we can note that based on the solutions (43) we already have the analytical solutions for the directional cosines $\gamma_i\ (i=1..3)$. However, it is needed to make some additional comments about the attitude of the magnetic DSSC.

Taking into account the components of the magnetic torque (13) we rewrite the vector equation (1) in the main carrier body frame $(\mathbf{\Omega}=\boldsymbol{\omega}_2)$ in the form

$$\dot{\mathbf{K}}+\boldsymbol{\omega}_2\times\mathbf{K}=\frac{B_{orb}}{K}\mathbf{m}\times\mathbf{K} \tag{45}$$

The equation (45) we can formally present as the vector equation of "the torque-free angular motion" considering the magnetic DSSC motion in the fictive coordinate frame rotating with the angular velocity $\tilde{\mathbf{\Omega}}$:

$$\dot{\mathbf{K}}+\tilde{\mathbf{\Omega}}\times\mathbf{K}=\mathbf{0} \tag{46}$$

$$\tilde{\mathbf{\Omega}}=\boldsymbol{\omega}_2-\frac{B_{orb}}{K}\mathbf{m} \tag{47}$$

However, for writing of the scalar equations system we can as before use the angular velocity parameters written in the projections onto the main body coordinate frame $Ox_2y_2z_2$; then for the fictive "torque-free" coordinate frame we have the following angular velocity

$$\tilde{\mathbf{\Omega}}_{Ox_2y_2z_2}=\left[p,q,r-Q/K\right]^T \tag{48}$$

In this case we take the fictive torque-free angular motion with conservation of the angular momentum and its projection onto "vertical" inertial axis OZ $\left(|\mathbf{K}|=K_{OZ}=K=\text{const}\right)$.

In the indicated "torque-free" coordinate frame we can write the well-known Poisson kinematical equations for the vector of the directional cosines $\boldsymbol{\gamma}=\left[\gamma_1,\gamma_2,\gamma_3\right]^T$ of the motionless "vertical" inertial axis OZ:

$$\dot{\boldsymbol{\gamma}}+\tilde{\mathbf{\Omega}}\times\boldsymbol{\gamma}=\mathbf{0} \tag{49}$$

So, based on the Poisson equation (49) and on the solutions (43) we will have the final exact analytical solutions for the directional cosines

$$\begin{aligned}&\gamma_1(t)=Ap(t)/K,\\&\gamma_2(t)=Bq(t)/K,\\&\gamma_3=\left(C_2r(t)+\Delta\right)/K\end{aligned} \tag{50}$$

Also, taking into account analytical solutions for the angular velocity components (43), by the full analogy with [12], in the considering case we can obtain exact solutions for the Euler angles (θ – the nutation angle, φ – the intrinsic rotation, ψ – the precession angle, δ – the relative rotation angle) as before considering the motion of the fictive "torque-free" coordinate frame (not the main carrier body frame) rotating with angular velocity $\tilde{\mathbf{\Omega}}$

$$\begin{aligned}&\cos\theta(t)=\left[C_2r(t)+\Delta\right]/K;\\&\operatorname{tg}\varphi(t)=\frac{Ap(t)}{Bq(t)}\end{aligned} \tag{51}$$

$$\begin{aligned}&\psi(t)-\psi_0=\int_{t_0}^{t}K\frac{Ap^2(t)+Bq^2(t)}{A^2p^2(t)+B^2q^2(t)}dt;\\&\delta(t)-\delta_0=\int_{t_0}^{t}\left(\frac{\Delta}{C_1}-r(t)\right)dt\end{aligned} \tag{52}$$

Figures 5 and 6 demonstrate the validity of the solutions (50) and (51) as the coincidence of the analytical results with the numerical integration.

It is needed to note that the numerical dependence for the intrinsic rotation angle (the green line at Fig.6) is continuous, but the analytical magnitude (51) of the intrinsic rotation angle (the blue color points at the Fig.6) is located into the interval $\left[-\pi/2\le\varphi\le\pi/2\right]$ in the full compliance with the actual range of the arctangent-function:

$$\varphi=\operatorname{arctg}\left(Ap(t)/\left(Bq(t)\right)\right).$$

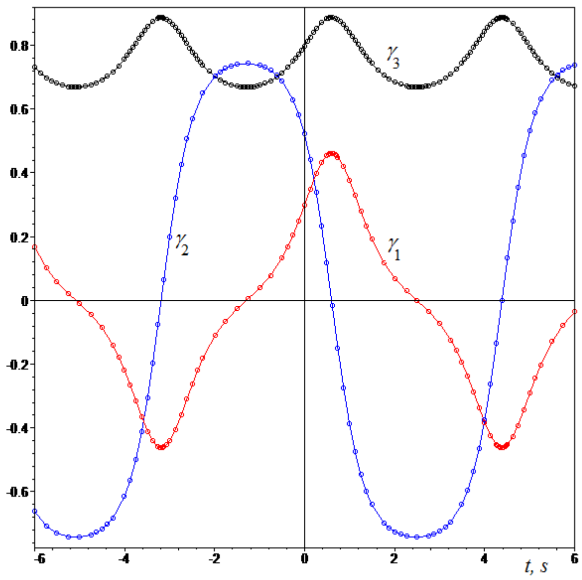

Fig.5 *The numerical integration (lines) and analytical (points) results for the directional cosines*
A_2=15, B_2=8, C_2=6, A_1=5, C_1=4 [kg·m^2];
p_0=0.75, q_0=2, r_0=5.83 [1/s];
$\Delta = 5$, K=50 [kg·m^2/s]; Q=100 [kg·m^2/s^2];
$\gamma_{10} = 0.3, \quad \gamma_{20} = 0.52, \quad \gamma_{30} = 0.8$

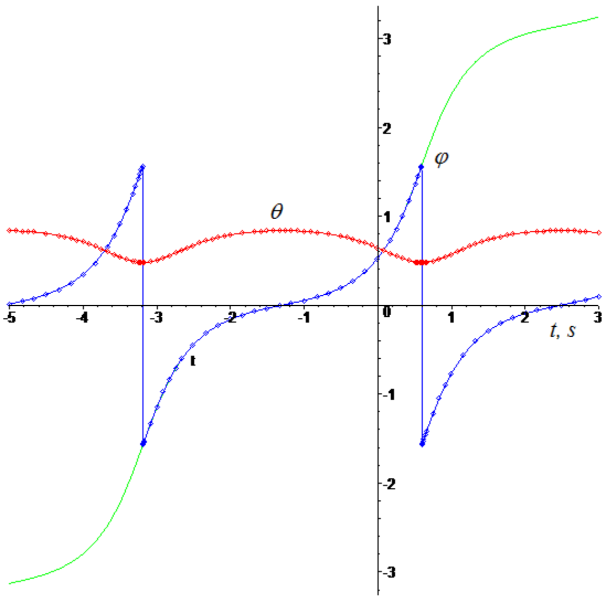

Fig.6 *The numerical integration (lines) and analytical (points) results for the Euler angles*
A_2=15, B_2=8, C_2=6, A_1=5, C_1=4 [kg·m^2];
p_0=0.75, q_0=2, r_0=5.83 [1/s];
$\Delta = 5$, K=50 [kg·m^2/s]; Q=100 [kg·m^2/s^2]
$\theta_0 = 0.64, \quad \varphi_0 = 0.52, \quad \psi_0 = 0.0$

By this reason we ought to add π to the analytical φ-value every rotational period.

Thus, the explicit exact analytical solutions are found for the attitude motion of the magnetic DSSC and for the angular motion of the coaxial bodies system with four degrees of freedom $\{p,q,r,\sigma,\psi,\theta,\varphi,\delta\}$. These unperturbed generating solutions can be used for the investigation of the perturbed motion problems, such as the angular motion of the DSSC with an electromagnetic equipment in the geomagnetic field, the orbital motion of a large DSSC with the account of the gravity gradient influence, and also the DSSC attitude dynamics in the resistant perturbed environment and with the chaotic behavior at the presence of small external/internal disturbances.

5 Conclusion

Dynamics of the magnetic DSSC (the coaxial bodies system) was examined in the case of the coincidence of the system angular momentum vector with the vector of the magnetic field (the "vertical" inertial axes for the corresponding Lagrange top). The new analytical solutions for the angular momentum components were obtained in terms of the Jacobi elliptic functions. The analytical solutions for the directional cosines and for the Euler angles were found. These essential analytical solutions can be used for the advanced analysis/synthesis of the dual-spin spacecraft attitude dynamics.

Also it is worth to note that the considered case of the magnetic DSSC attitude motion under the influence of the restoring/overturning magnetic torque can be characterized as the continuation of the generalization of the classical Lagrange top (and the coaxial Lagrange top [39]). At the same time this motion case can be directly reduced to the torque-free DSSC motion and to the previous results [12] at zero-value of the magnetic torque – it can be characterized as the generalization of the Euler case of the torque-free DSSC motion. Due to the similarity of the DSSC attitude dynamics with the torque-free coaxial bodies' rotational motion as well as with the precession motion of the magnetic coaxial system (in the particular case of the coincidence of the magnetic field vector and the system angular momentum) the "dynamical equivalence" between the gyroscopic and magnetic DSSC attitude stabilization at the orbital motion along the circular equatorial orbit takes place.

So, on the one hand, the considered dynamics of the magnetic DSSC is connected with the fundamental classical tasks (the Lagrange and the Euler tops); and, on the other hand, the studied coaxial system represents the important practical application of spaceflight dynamics.

Acknowledgements:
This research was supported by Russian Foundation for Basic Research (RFBR # 11-08-00794-a).

References:

[1] V. Volterra, Sur la théorie des variations des latitudes. Acta Math. 22 (1899).

[2] N.E. Zhykovski, On the motion of a rigid body with cavities filled with a homogeneous liquid. Collected works, V.1, Moscow-Leningrad, Gostekhisdat, 1949.

[3] J. Wittenburg, Dynamics of Systems of Rigid Bodies. Stuttgart: Teubner, 1977.

[4] J. Wittenburg, Beitrage zur dynamik von gyrostaten, Accademia Nazional dei Lincei, Quaderno N. 227 (1975) 1–187.

[5] V.V. Golubev, Lectures on Integration of the Equations of Motion of a Rigid Body about a Fixed Point, State Publishing House of Theoretical Literature, Moscow, 1953.

[6] V.V. Kozlov, Methods of qualitative analysis in the dynamics of a rigid body, Gos. Univ., Moscow, 1980.

[7] A. Elipe, V. Lanchares, Exact solution of a triaxial gyrostat with one rotor, Celestial Mechanics and Dynamical Astronomy, Issue 1-2, Volume 101, 2008, pp 49-68.

[8] I. Basak, Explicit solution of the Zhukovski-Volterra gyrostat, Regular and chaotic dynamics Vol.14, N.2 (2009) 223-236.

[9] E.A. Ivin, Decomposition of variables in task about gyrostat motion. Vestnik MGU (Transactions of Moscow's University). Series: Mathematics and Mechanics. No.3 (1985) Pp. 69-72.

[10] V.S. Aslanov, Spatial Motion of a Body at Descent in the Atmosphere [in Russian], Moscow:·Fizmatlit, 2004, 160 p.

[11] V.S. Aslanov, Integrable cases in the dynamics of axial gyrostats and adiabatic invariants, Nonlinear Dynamics, Volume 68, Numbers 1-2 (2012) 259-273.

[12] A.V. Doroshin, Exact solutions for angular motion of coaxial bodies and attitude dynamics of gyrostat-satellites, International Journal of Non-linear Mechanics 50 (2013) 68-74.

[13] H. Andoyer, Cours de Mecanique Celeste, Paris: Gauthier-Villars, 1924.

[14] A. Deprit, A free rotation of a rigid body studied in the phase plane, American Journal of Physics 35 (1967) 425 – 428.

[15] P. J. Holmes, J. E. Marsden, Horseshoes and Arnold diffusion for Hamiltonian systems on Lie groups, Indiana Univ. Math. J. 32 (1983) 283-309.

[16] C.D. Hall, R.H. Rand, Spinup Dynamics of Axial Dual-Spin Spacecraft, Journal of Guidance, Control, and Dynamics, Vol. 17, No. 1 (1994) 30–37.

[17] C.D. Hall, Momentum Transfer Dynamics of a Gyrostat with a Discrete Damper, Journal of Guidance, Control, and Dynamics, Vol. 20, No. 6 (1997) 1072-1075.

[18] A.I. Neishtadt, M.L. Pivovarov, Separatrix crossing in the dynamics of a dual-spin satellite. Journal of Applied Mathematics and Mechanics, Volume 64, Issue 5, 2000, Pages 709-714.

[19] A.V. Doroshin, Chaos and its avoidance in spinup dynamics of an axial dual-spin spacecraft. Acta Astronautica, Volume 94, Issue 2, February 2014, Pages 563-576.

[20] M. Inarrea, V. Lanchares, Chaos in the reorientation process of a dual-spin spacecraft with time-dependent moments of inertia, Int. J. Bifurcation and Chaos. 10 (2000) 997-1018.

[21] A.V. Doroshin, Evolution of the precessional motion of unbalanced gyrostats of variable structure. Journal of Applied Mathematics and Mechanics, Volume 72, Issue 3, October 2008, Pages 259-269.

[22] A.V. Doroshin, M.M. Krikunov, Attitude Dynamics of a Spacecraft with Variable Structure at Presence of Harmonic Perturbations, Appl. Math. Modelling (2013), doi: http://dx.doi.org/10.1016/j.apm.2013.10.021

[23] R. Molina, F. Mondéjar, Equilibria and stability for a gyrostat satellite in circular orbit, Acta Astronautica, Volume 54, Issue 2 (2004) 77-82.

[24] Jinlu Kuang, Soonhie Tan, Kandiah Arichandran, A.Y.T. Leung, Chaotic dynamics of an asymmetrical gyrostat, International Journal of Non-Linear Mechanics, Volume 36, Issue 8 (2001) 1213-1233.

[25] Awad El-Gohary, Chaos and optimal control of steady-state rotation of a satellite-gyrostat on a circular orbit, Chaos, Solitons & Fractals, Volume 42, Issue (2009) 2842-2851.

[26] V.A. Bushenkov, M. Yu. Ovchinnikov, G.V. Smirnov, Attitude stabilization of a satellite by magnetic coils, Acta Astronautica, Volume 50, Issue 12 (2002) 721-728

[27] M.Yu. Ovchinnikov, D.S. Roldugin, V.I. Penkov, Asymptotic study of a complete magnetic attitude control cycle providing a single-axis orientation, Acta Astronautica 77 (2012) 48–60

[28] Yan-Zhu Liua, Hong-Jie Yu, Li-Qun Chen, Chaotic attitude motion and its control of spacecraft in elliptic orbit and geomagnetic field, Acta Astronautica 55 (2004) 487 – 494.

[29] Li-Qun Chen, Yan-Zhu Liu, Chaotic attitude motion of a magnetic rigid spacecraft and its control, International Journal of Non-Linear Mechanics 37 (2002) 493–504.

[30] Li-Qun Chen, Yan-Zhu Liu, Gong Cheng, Chaotic attitude motion of a magnetic rigid spacecraft in a circular orbit near the equatorial plane, Journal of the Franklin Institute 339 (2002) 121–128.

[31] M. Lovera, A. Astolfi, Global Magnetic Attitude Control of Spacecraft in the Presence of Gravity Gradient, IEEE Ttansactions On Aerospace And Electronic Systems, Vol. 42, No. 3 (2006) 796-805.

[32] M. Lovera, A. Astolfi, Spacecraft attitude control using magnetic actuators, Automatica 40 (2004) 1405 – 1414.

[33] Enrico Silani, Marco Lovera, Magnetic spacecraft attitude control: a survey and some new results, Control Engineering Practice 13 (2005) 357–371.

[34] A.V. Doroshin, Synthesis of attitude motion of variable mass coaxial bodies, WSEAS Transactions on Systems and Control, Issue 1, Volume 3 (2008) 50-61.

[35] A.V. Doroshin, Analysis of attitude motion evolutions of variable mass gyrostats and coaxial rigid bodies system, International Journal of Non-Linear Mechanics, Volume 45, Issue 2 (2010) 193–205.

[36] A.V. Doroshin, Modeling of chaotic motion of gyrostats in resistant environment on the base of dynamical systems with strange attractors. Communications in Nonlinear Science and Numerical Simulation, Volume 16, Issue 8 (2011) 3188–3202.

[37] V.S. Aslanov, A.V. Doroshin, Chaotic dynamics of an unbalanced gyrostat. Journal of Applied Mathematics and Mechanics, Volume 74, Issue 5 (2010) 525-535.

[38] A.V. Doroshin, Heteroclinic dynamics and attitude motion chaotization of coaxial bodies and dual-spin spacecraft, Communications in Nonlinear Science and Numerical Simulation, Volume 17, Issue 3 (2012) 1460–1474.

[39] V.S. Aslanov and A.V. Doroshin, Two cases of motion of an unbalanced gyrostat, Mech. Solids. 41 (4), 29-39 (2006).

[40] C. F. de Melo and O. C. Winter, Alternative Paths To Earth-Moon Transfer, Mathematical Problems in Engineering, Volume 2006, Article ID 34317, Pages 1–20, DOI 10.1155/MPE/2006/34317.

[41] Filippo Neri, Traffic packet based intrusion detection: decision trees and generic based learning evaluation. WSEAS Transactions on Computers, WSEAS Press (Wisconsin, USA), issue 9, vol. 4, 2005, pp. 1017-1024.

[42] Filippo Neri, Software agents as a versatile simulation tool to model complex systems. WSEAS Transactions on Information Science and Applications, WSEAS Press (Wisconsin, USA), issue 5, vol. 7, 2010, pp. 609-618.

[43] L. Nechak, S. Berger, E. Aubry, Robust Analysis of Uncertain Dynamic Systems: Combination of the Centre Manifold and Polynomial Chaos theories, WSEAS TRANSACTIONS on SYSTEMS, Issue 4, Volume 9, April 2010, pp.386-395.

[44] N. Jabli, H. Khammari, M. F. Mimouni, R. Dhifaoui, Bifurcation and chaos phenomena appearing in induction motor under variation of PI controller parameters, WSEAS TRANSACTIONS on SYSTEMS, Issue 7, Volume 9, July 2010, pp.784-793.

[45] Thanh Dung Nguyen, Thi Thanh Dieu Phan, Roman Jasek, Parameter Estimation in Five Dimensions Chaotic Synchronization Systems by Self-Organizing Migrating Algorithm, WSEAS TRANSACTIONS on SYSTEMS, Issue 4, Volume 11, April 2012, pp.117-128.